



## Speciation across mountains: Phylogenomics, species delimitation and taxonomy of the *Liolaemus leopardinus* clade (Squamata, Liolaemidae)

Damien Esquerré<sup>a,\*</sup>, Diego Ramírez-Álvarez<sup>b</sup>, Carlos J. Pavón-Vázquez<sup>a</sup>, Jaime Troncoso-Palacios<sup>c</sup>, Carlos F. Garín<sup>d,e</sup>, J. Scott Keogh<sup>a</sup>, Adam D. Leaché<sup>f</sup>

<sup>a</sup> Division of Ecology and Evolution, Research School of Biology, The Australian National University, Canberra, ACT, Australia

<sup>b</sup> Servicio Agrícola y Ganadero de Chile, Región de O'Higgins, Rancagua, Chile

<sup>c</sup> Laboratorio de Fisiología y Biofísica, Facultad de Medicina, Universidad de Chile, Santiago, Chile

<sup>d</sup> Universidad Andrés Bello, Departamento de Ecología y Biodiversidad, Facultad de Ciencias de la Vida, República 440, Santiago, Chile

<sup>e</sup> Instituto de Ecología y Biodiversidad (IEB), Santiago, Chile

<sup>f</sup> Department of Biology & Burke Museum of Natural History and Culture, University of Washington, Seattle, WA, USA

### ARTICLE INFO

#### Keywords:

Species delimitation  
Lizards  
Andes  
SNPs  
ddRADseq  
Phylogenomics

### ABSTRACT

Organisms rapidly diversifying across unstable environments such as mountain tops provide substantial challenges for resolving evolutionary histories and delimiting species. The *Liolaemus leopardinus* clade is a group of five species of lizards adapted to high altitudes in central Chile, with most species found in the Andes, but one species, *L. frassinettii* is found in the independent Costa Cordillera. Despite their allopatric distributions, they display shallow mitochondrial divergences, making phylogenetics and species delimitation of this clade hard to resolve. We use an integrative approach to delimit species by considering morphological data (linear and landmark-based), mitochondrial DNA (mtDNA), and nuclear DNA (Sequences and SNPs collected with ddRADseq). We find strong conflicting signals between phylogenetic analyses of the nuclear and mtDNA data. While mtDNA places *L. frassinettii* as sister to the rest of the clade, the SNPs support a south to north order of divergences, with southernmost species (new taxon described here) as sister to the rest of the clade. Moreover, species delimitation using mtDNA only supports two species (one in the Costa and one in the Andes), whereas combined analyses using the nuclear data and morphology support multiple Andean taxa, including a new one we describe here. Based on these results, population structure analyses and our knowledge of the geological and climatic history of the Andes, we argue that this mito-nuclear discordance is explained by past introgression among the Andean taxa, likely during glacial periods that forced these lizards to lower altitudes where they would hybridize. The complete isolation between the Costa and Andes cordilleras has prevented any further contact between taxa on either mountain chain. Our study highlights the importance of using multiple lines of evidence to resolve evolutionary histories, and the potential misleading results from relying solely on mtDNA.

### 1. Introduction

The field of taxonomy is moving towards a more integrative approach which takes account of different lines of evidence to delimit species (Dayrat, 2005). The rapid advance of genomic data acquisition, coupled with better understanding of speciation processes, has made species delimitation much more quantitative (Fujita et al., 2012). Nonetheless, reconciling differences between morphology and genetics can still be challenging in situations where they disagree. For example, species with deep divergences can remain morphologically indistinguishable due to static selective pressures or niche conservatism, resulting in morphologically cryptic species (Boumans et al., 2007;

Murphy et al., 2016; Padial and la Riva, 2009; Welton et al., 2013). At the other extreme, populations of the same species can display substantial morphological divergence due to local adaptation, phenotypic plasticity or other evolutionary mechanisms (Keogh et al., 2005; Weitschat, 2016). Figuring out how to resolve discrepancies between genetics and morphology is difficult but necessary for taxonomic progress.

Recent speciation can produce complex species delimitation problems due to high levels of incomplete lineage sorting and introgression (Grummer et al., 2018; Olave et al., 2018; Shaffer et al., 2007). Rapidly changing geological systems like volcanic islands (Givnish et al., 2009), many lake systems (April et al., 2013; Near and Benard, 2004) and

\* Corresponding author.

E-mail address: [damien.esquerre@anu.edu.au](mailto:damien.esquerre@anu.edu.au) (D. Esquerré).

<https://doi.org/10.1016/j.ympev.2019.106524>

Received 9 November 2018; Received in revised form 14 February 2019; Accepted 29 May 2019

Available online 03 June 2019

1055-7903/© 2019 Elsevier Inc. All rights reserved.

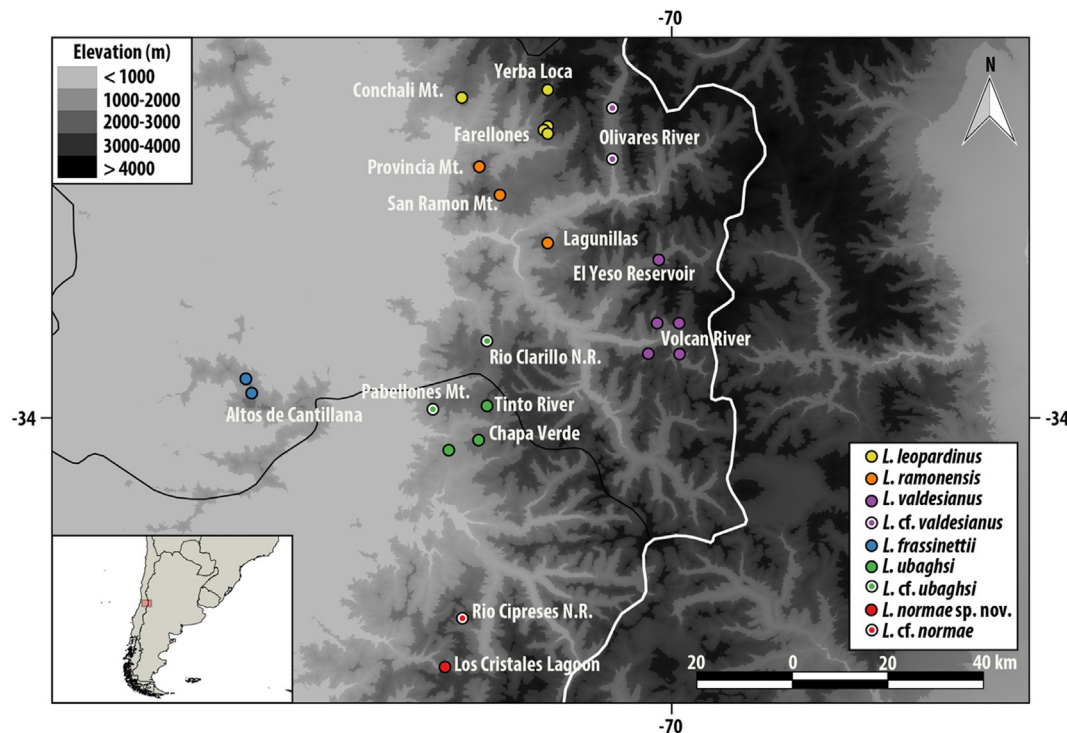


Fig. 1. Altitudinal map displaying the samples and known records included in this study. Populations are assigned to species according to the legend on the bottom right. Points with a white circle inside indicate records for which there are only photographs and no specimens have been collected or examined. The white line represents the border between Chile (West) and Argentina (East) and the black line the division between the Metropolitan (North) and O'Higgins (South) regions of Chile.

forming cordilleras (Vuilleumier, 1970) are commonly home to such systems. Emergence of these isolated habitats can drive populations to allopatry over relatively short periods of time. Mountain tops can act as biological islands for species adapted to high altitudes (i.e. sky islands), and are increasingly recognized as generators of biodiversity (Lagomarsino et al., 2016; Sedano and Burns, 2010; Spehn et al., 2011). The Andes Cordillera in South America is one of the most violently uplifting mountain chains in the world (Garzone et al., 2014; Gregory-Wodzicki, 2000), and it acts as a species pump for a diverse array of taxa (Aleixo and de Fátima Rossetti, 2007; Esquerré et al., 2019; Hughes and Eastwood, 2006).

*Liolaemus* lizards are a diverse radiation of 260 species (Abdala and Quinteros, 2014; Uetz and Hošek, 2014). They are inferred to have started diversifying in the late Oligocene (Esquerré et al., 2019) and they display a biogeographic and diversification history closely linked to the Andes (Díaz-Gómez, 2011; Esquerré et al., 2019; Pincheira-Donoso et al., 2013; Portelli and Quinteros, 2018; Schulte et al., 2000). This group includes clades well adapted to many different environments throughout the southern half of South America. Among them, the *Liolaemus elongatus-kriegi* complex comprises 34 viviparous species (see Supporting Information for list) adapted to the cold climates of the Andes and Patagonia between Chile and Argentina (Cei, 1974; Morando et al., 2003; Uetz and Hošek, 2014). The taxonomy of this group is unstable and unresolved due partly to a 350% increase in taxonomic diversity in the last 20 years (e.g. Abdala et al., 2010; Avila et al., 2015; Esquerré et al., 2013; Medina et al., 2017; Troncoso-Palacios et al., 2015). Within this complex, the *Liolaemus leopardinus* clade is particularly interesting from a species delimitation perspective. They are all high-altitude species with allopatric populations found between 1500 and around 3000 m above the sea level and they tend to share a leopard-like dorsal pattern, which gives them the name of 'leopard lizards' (Esquerré and Núñez, 2017). They are a very young group, only 1–3 million years old (Esquerré et al., 2019), and preliminary analyses recover extremely shallow mitochondrial divergences (Esquerré et al.,

2014). These contrasting features of isolated populations with distinct phenotypes, but low mitochondrial divergence, make this system ideal for integrative species delimitation approaches.

For a long time, *Liolaemus leopardinus* comprised three subspecies, all from the Andean mountain range of central Chile (Donoso-Barros, 1966; Hellmich, 1950; Müller and Hellmich, 1932): *Liolaemus leopardinus leopardinus* Müller and Hellmich, 1932, *L. leopardinus ramonensis* Müller and Hellmich, 1932 and *L. leopardinus valdesianus* Hellmich, 1950. These taxa were raised to full species based on karyotypes and morphological differences (Núñez and Jaksic, 1992; Pincheira-Donoso and Núñez, 2005), but little other work was done on this group since (but see Espejo, 1989; Espejo et al., 1987; Navarro and Diaz, 1986). The much later discovery and description of *L. frassinettii* Núñez, 2007, a species found in the Costa Cordillera mountain chain that runs parallel to the Andes along central Chile, and the description of *L. ubaghsi* Esquerré, Troncoso-Palacios, Garín, Núñez (2014), from the most southern known population of leopard lizards, increased the number of species in the group to five and re-ignited an interest in the diversity and evolution of this group (Esquerré et al., 2014; Núñez, 2007). Further exploration of the Andes south of Santiago have resulted in the discovery of new populations including one that displays a unique phenotype in Los Cristales Lagoon, O'Higgins Region. A detailed taxonomic revision of the group can be found in Esquerré et al. (2014).

Establishing phylogenetic relationships and species boundaries in rapidly diversifying organisms like *Liolaemus* remains challenging. Recent studies have found high levels of incomplete lineage sorting and introgression (Grummer et al., 2018; Olave et al., 2018). Using molecular data drawn from independently evolving regions of the genome is therefore necessary to incorporate the variation in gene histories from different loci (Fujita et al., 2012; Grummer et al., 2014; Nieto-Montes de Oca et al., 2017). These approaches, combined with morphological data and the current knowledge on past geological and climatic events, provided us an integrative framework to elucidate the enigmatic evolution of the leopard lizards of the Andes.

## 2. Materials and methods

### 2.1. Taxonomic sampling

We included 98 samples from 20 localities of the *Liolaemus leopardinus* clade (*sensu* (Esquerré et al., 2014)) (Table S1). These include *L. leopardinus*, *L. ramonensis*, *L. valdesianus*, *L. ubaghsi*, *L. frassinettii* and a population that possibly represents an undescribed taxon from Los Cristales Lagoon, O'Higgins Region, Chile (see Fig. 1). We additionally added samples of *L. curis* which appears to be the sister lineage to the *L. leopardinus* clade (Esquerré et al. in prep.) and *Liolaemus elongatus* from the Araucanía Region of Chile (for mtDNA only). The specimens are located in the Museo Nacional de Historia Natural de Chile (MNHN) and the Colección de Flora y Fauna, Profesor Patricio Sánchez Reyes of the Pontificia Universidad Católica de Chile (SSUC).

### 2.2. Morphometric sampling

We measured 88 specimens from almost all known localities of all the species in the *Liolaemus leopardinus* clade (see Table S1). We focused on three aspects of the phenotype: body shape, head shape in dorsal view and head shape in lateral view. For body shape representation, we used linear morphometrics. We measured snout-vent length (SVL) as a proxy for body size and recorded 25 other morphometric measurements: axilla-groin distance (AGD), tail length (TL), foot length, tibial length, femoral length, humeral length, radial length, hand length, head length, head width, head depth, rostral scale width, rostral scale height, internarial distance, inter-eye distance, ear-eye distance, loreal length, eye length, neck width, ear opening width and ear opening height. All these measurements were done with a digital caliper and performed by the same person (DE) to avoid bias. Additionally, we recorded six meristic scale count characters: scales around mid-body, dorsal scales, ventral scales, third finger lamellae, third toe lamellae and fourth toe lamellae. Details on the measurements can be seen in Fig. 2. Missing tail lengths (cut or regenerated) were imputed for some specimens with the function *imputePCA* from the R package *MissMDA* (Josse and Husson, 2012). For head shape, we used geometric morphometrics. We took dorsal and lateral photographs of the head of each specimen using a Canon 7D camera with a Canon 60 mm f/2.8 macro lens and a Canon Twin Lite MT 24-Ex macro flash. A scale-bar was used in each photograph to quantify size. To characterize head shape in dorsal view we used 10 landmarks and 12 semi-landmarks and for the lateral view we used eight landmarks (Fig. 2). These were digitized using *tpsDig v.2.17* (Rohlf, 2015). Semilandmarks were allowed to slide to minimize bending energy (Gunz and Mitteroecker, 2013) on *tpsRelw v.1.54* (Rohlf, 2015). To remove the effects of location, scale and orientation, and thus only retaining shape information we used a generalized Procrustes analysis (Rohlf and Slice, 1990). We took object symmetry into account for the dorsal view, using the function *bilat.symmetry* in the R package *geomorph 3.0* (Adams et al., 2016).

### 2.3. Morphometric analyses

We wanted to quantify the degree of shape and not size variation, therefore we needed to remove the effect of size or scale, while maintaining allometric variation (Esquerré et al., 2017; Klingenberg, 2016). For the geometric morphometric data, this is done during generalized Procrustes analysis. For the linear body measurements we used log-shape ratios (Claude, 2013; Mosimann and James, 1979), which are obtained by computing size as the geometric mean of all the measurements (for each specimen) and then dividing each variable by this measure of size and log-transforming it. We then proceeded to test the effect of sex and species on shape by fitting a linear model with the function *procDlm* from the R package *geomorph*, and testing the significance with a residual randomization procedure of 10,000 iterations. To identify individual differences between pairs of species we

performed pairwise comparisons using the function *advanced.procD.lm* in *geomorph*. To visualize the shape variation, we performed principal component analyses (PCA) on the shape data. For body shape data, we used the function *PCA* from the R package *FactoMineR* (Lê et al., 2008), and for head shape data we used the function *plotTangentspace* from *geomorph*.

### 2.4. Molecular sampling

We obtained sequences for mitochondrial genes cytochrome *b* (*cytb*) and cytochrome *c* oxidase subunit I (*COI*) for 30 individuals of the *Liolaemus leopardinus* clade plus five individuals of *L. curis* and three of *L. elongatus*. For *cytb* the fragment was amplified via Polymerase Chain Reaction (PCR) using the IguacCytob F2 and IguacCytob R2 primers (Corl et al., 2010) under the following thermocycling conditions: denaturation at 94 °C for 5 min, then cycle 35 times at 94 °C for 30 s, 50 °C for 30 s, 72 °C for 1.5 min, and then a final hold at 72 °C for 5 min. Sequencing reactions were performed with a Big Dye Kit (Applied Biosystems, Foster City, CA). Sequencing was done on an ABI 3130xl Genetic Analyzer. Sequences were then edited on Geneious 9.0.4 (Biomatters, Auckland, New Zealand, 2015). The *COI* fragment was amplified and sequenced by the Cold Code initiative for barcoding amphibians and non-avian reptiles (Murphy et al., 2013).

For nuclear data, we sequenced 17 samples using ddRADseq (Peterson et al., 2012) to collect SNPs (Single Nucleotide Polymorphisms). SNPs have been increasingly used in phylogenetic and species delimitation studies due to their advantages over other, costlier genomic approaches (Leaché and Oaks, 2017). SNPs are particularly appealing due to their high informative content across the nuclear genome, particularly when dealing with shallow divergences where nuclear exons may provide less variation (Harvey et al., 2016). RADSeq methods also provide information on genetic variation from hundreds to thousands of independent loci, which has an increasingly recognized importance in phylogenetic and phylogeographic studies (Harvey et al., 2016). Our library preparation methods followed those used in other studies of lizard phylogeography and species delimitation (Leaché et al., 2017; Nieto-Montes de Oca et al., 2017; Richmond et al., 2017). Briefly, we double-digested DNA using the restriction enzymes *SbfI* and *MspI*, followed by bead purification and ligation of barcoded Illumina adaptors, size-selection, and library quantification. Samples were sequenced on a single Illumina HiSeq 4000 lane (50-bp, single-end reads) at the QB3 Genome Sequencing facility at the University of California, Berkeley.

For the processing of raw reads, including demultiplexing, filtering, clustering, phasing and alignment files generation we used the program *ipyRAD v.0.7.19* (Eaton and Overcast, 2016). We demultiplexed the samples using their unique barcode and adapter sequences, which after being removed, each locus was reduced from 50 to 39 bp. Details for the parameters used for the assembly can be seen in the Supplementary Data File 1. The final dataset included 5116 loci and contained 8542 SNPs. Since some analyses are more sensitive to missing data, we additionally performed a SNP assembly allowing for no missing data, which resulted in a dataset of 1117 loci and 1997 SNPs. For reference, we will refer to these two datasets to the full and reduced datasets, respectively. Finally, using the R package *phrynomics* (Leaché et al., 2015), we filtered the loci to only include unlinked (one SNP per locus), biallelic sites and exported them in different formats to be used in the analyses described below. We refer to this dataset as the unlinked biallelic data. For more specific filtering and transformation we used *PGDSpider v. 2.1.1.3* (Lischer and Excoffier, 2012), R v. 3.4.0 (R Core Team, 2017), *TriFusion v. 1.0.0* (<https://github.com/OdiogoSilva/TriFusion>), and the bash command line.

### 2.5. Phylogenetic hypotheses

The mitochondrial sequences for *cytb* and *COI* were concatenated

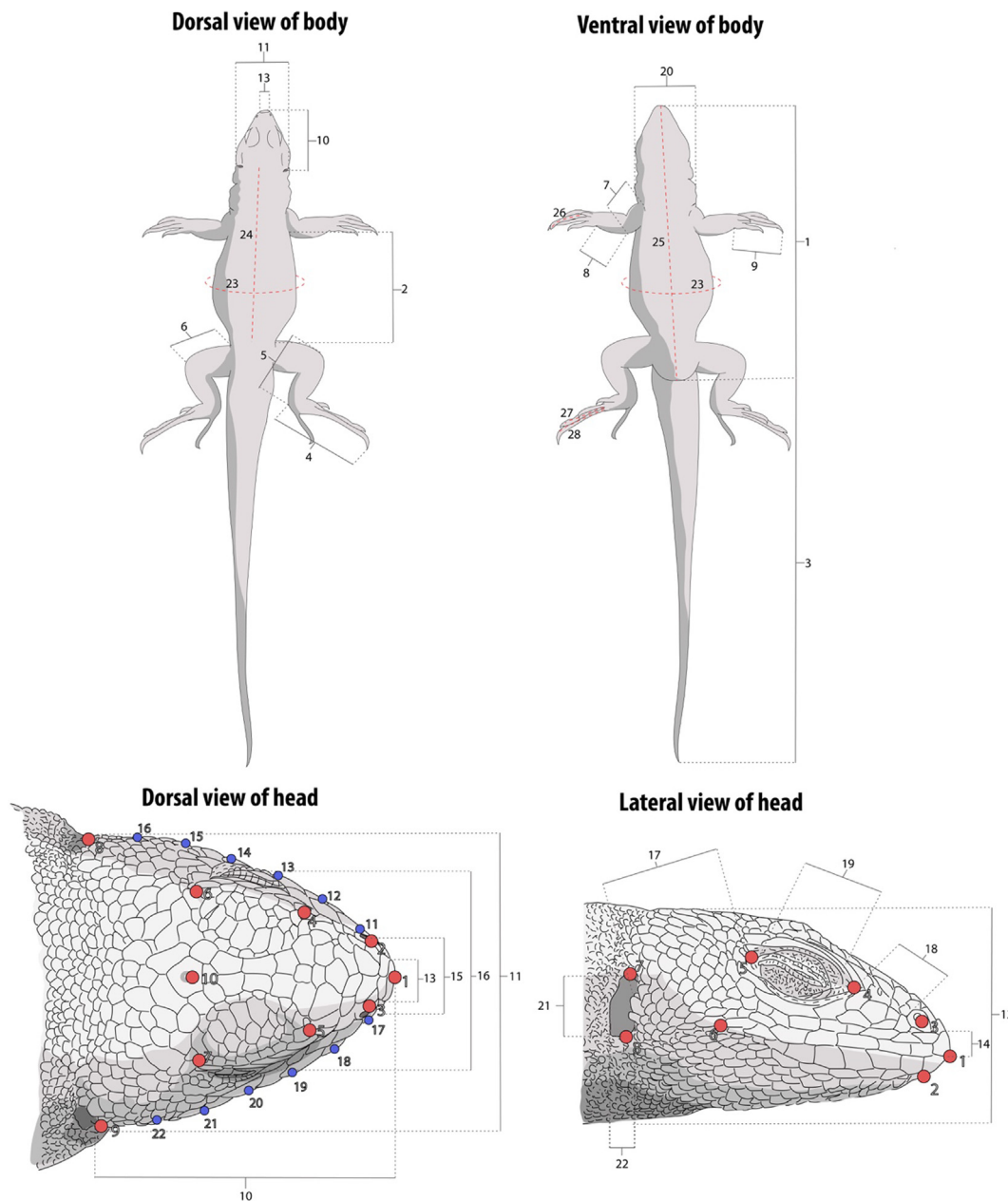


**Fig. 2.** Morphological data taken from body and head shape of the specimens. Small numbers correspond to the following measurements: 1, SVL; 2, AGD; 3, TL; 4, foot length; 5, tibial length; 6, femoral length; 7, humeral length; 8, radial length; 9, hand length; 10, head length; 11, head width; 12, head depth; 13, rostral scale width; 14, rostral scale height; 15, internarial distance; 16, inter-eye distance; 17, ear-eye distance; 18, loreal length; 19, eye length; 20, neck width; 21, ear opening width; 22, opening height; 23, scale count characters scales around mid-body; 24, dorsal scales; 25, ventral scales; 26, third finger lamellae; 27, third toe lamellae; 28, fourth toe lamellae. Red dashed lines indicate scale counts. The head illustrations show the landmarks (big red dots) and semi-landmarks (small blue dots) used to describe head shape variation. (For interpretation of the references to color in this figure legend, the reader is referred to the web version of this article.)

using Geneious 9.0.4 (Biomatters, Auckland, New Zealand, 2015), aligned with MAFFT v.7.309 (Katoh and Standley, 2013) and checked by eye. We used PartitionFinder 2 (Lanfear et al., 2016) to find the best gene partitioning scheme and substitution model for each partition using the Bayesian information criterion (BIC), with the dataset partitioned by gene and by codon position. The program found both mitochondrial genes as one single partition evolving under the HKY + G substitution model. We performed a Bayesian phylogenetic analysis using BEAST v.2.4.7 (Bouckaert et al., 2014). We used a strict molecular clock and a Yule speciation model for the branching pattern of the trees. We ran four independent Markov chain Monte Carlo (MCMC) chains for 100 million generations. We assessed that the chains had proper mixing and convergence with Tracer v.1.6.0 (Rambaut et al., 2014) and RWTY

v.1.0.1 (Warren et al., 2017), confirming minimum effective sample size (ESS) of over 200 for every parameter including tree topology. We combined the results of the chains and discarded the first 20% of each run as burn in with LogCombiner v.2.4.2 and summarized a maximum clade credibility (MCC) tree keeping the median heights on TreeAnnotator v.2.4.2. To infer a maximum likelihood (ML) tree we used RAxML v.8.2 (Stamatakis, 2014) with the GTRGAMMA substitution model and 1000 rapid bootstrap replicates.

We used three different approaches to analyse the nuclear data in a phylogenetic context. First, we used a concatenated alignment of the full ddRADseq loci without removing the constant sites to avoid acquisition bias resulting in overestimation of branch lengths and potentially wrong topological inference (Leaché et al., 2015). We

performed this analysis using RAxML with the same specifications as above. Second, we used the unlinked biallelic data to infer a species tree under the multi-species coalescent model using the program SVDQuartets (Chifman and Kubatko, 2014), implemented in PAUP v. 4 (Swofford, 2003), which infers four-taxon relationships (quartets) based on the SNP patterns. We estimated branch support by performing 1000 bootstrap replicates. We performed one analysis with all specimens as independent samples and one where we assigned them to taxon partitions. Finally, we estimated a Bayesian species tree using the program SNAPP version 1.3 (Bryant et al., 2012), implemented in BEAST 2. This program estimates species trees by modeling the probability of allele frequency changes between ancestor and descendant nodes directly from biallelic data. For this analysis, we used the reduced unlinked SNPs. We set the mutation rates  $U$  and  $V$  to 1 and sampled the coalescence rate through the MCMC. The expected divergence ( $\theta$ ) prior was set according to the mean divergence within populations, using a gamma distribution with  $\alpha = 1$  and  $\beta = 70$ . The speciation rate ( $\lambda$ ) prior was set according to the maximum observed sequence divergence between any two taxa, using a gamma distribution with  $\alpha = 2$  and  $\beta = 200$ . The MCMC chain was set to 1.5 million generations, sampling every 1000 steps. Each model was run twice to ensure consistent results and we confirmed that the ESS for each step was higher than 200. We discarded the first 20% of each run as burn in and combined the results of the chains with LogCombiner. We summarized a maximum clade credibility (MCC) tree using the median node heights in TreeAnnotator.

## 2.6. Species delimitation

Most modern taxonomists agree that species are independently evolving metapopulation lineages (De Queiroz, 2007; de Queiroz, 1998), but diagnosing such entities remains an issue. We take a total evidence approach and analyze as many lines of evidence as possible to delimit species, since the accumulation of evidence should provide stronger support for species status (de Queiroz, 2007). To delimit species in the *L. leopardinus* clade, we combine morphological, genetic (nuclear and mtDNA), ecological, and geographic information.

For single locus species delimitation using the mtDNA data, we used the Generalized Mixed Yule Coalescent (GMYC) model using the *gmyc* function from the R package *splits* (Fujisawa and Barraclough, 2013) and using the *single threshold* option. The GMYC model works under a likelihood framework to find the best model of branching considering a Yule pure-birth process of between species diversification and a neutral coalescent process of branching for within species diversification, finding the transition points to speciation events using a fully resolved ultrametric tree (Fujisawa and Barraclough, 2013; Pons et al., 2006). We also used the multi-rate Poisson Tree Process (mPTP) (Kapli et al., 2016) which models intra and interspecific processes based on the number of molecular substitutions on branches, and therefore does not require an ultrametric tree. For the GMYC analysis we used the MCC tree from our BEAST analysis, and for the mPTP analysis we used the RAxML phylogeny.

To perform species delimitation using the ddRADseq data we used four approaches. First, we performed Bayes Factors species delimitation or BFD\* (Leaché et al., 2014) using SNAPP with the parameters described above. We used the assembly with no missing data to avoid overestimating the number of species (Leaché et al., 2018a). To estimate the marginal likelihood of each species delimitation model we conducted a stepping stone analysis ( $\alpha = 0.3$ ) using 48 steps with an MCMC length of 200,000 generations and a pre-burnin of 50,000. We ran two independent analyses per species delimitation model (see Table 1). We ranked the species delimitation models by their marginal likelihoods and calculated the Bayes Factors to compare the models (Kass and Raftery, 2012).

For the second approach, we used the program BPP v. 3.3 (Yang, 2015; Yang and Rannala, 2010). We used the phased sequences

generated with ddRADseq as input. Mixing issues occurred when estimating the species tree and species limits jointly, when using a high number of loci, and when considering each of the described species (*L. frassinettii*, *L. leopardinus*, *L. ramonensis*, *L. valdesianus*, and *L. ubaghsi*) and the sample from Los Cristales Lagoon as distinct putative species. After trying different combinations of input data and priors, we settled for the combinations described below. We fixed the species tree topology in all the analyses based on the species tree estimated with SVDQuartets. Support values and resolution for the interspecific relationships were high in that tree except for the relationship between *L. leopardinus* and *L. ramonensis* (see Results). We deleted loci with missing data (excluding gaps) from the alignment and conducted three BPP analyses: one including 30 loci and considering each described species and the sample from Los Cristales Lagoon as distinct putative species; one including 300 loci, considering *L. leopardinus*, *L. ramonensis* and *L. valdesianus* as a single species, and considering each of the remaining species and the sample from Los Cristales Lagoon as distinct putative species; and one including 300 loci, considering *L. leopardinus*, *L. ramonensis* and *L. valdesianus* as distinct putative species, and excluding the remaining samples from the analysis. The MCMC of the first and third analyses consisted of a burnin period of 40,000 iterations and a post-burnin period of 10 million iterations sampled every fifth iteration. The second analysis consisted of a burnin period of 10,000 iterations and a post-burnin period of 2.5 million iterations sampled every fifth iteration. We ran each analysis twice to verify the consistency between runs. The ancestral population size ( $\theta$ ) and root age ( $\tau$ ) priors were assigned the gamma distributions  $G(1, 10)$  and  $G(2, 2000)$  in all the analyses, respectively. This combination of priors is considered conservative, as it represents large ancestral population sizes and shallow divergences (Leaché and Fujita, 2010; Yang, 2015).

For our third species delimitation approach, we incorporated our phenotypic data using the program iBPP v. 2.1 (Solís-Lemus et al., 2015). This program uses the same framework as described above for BPP but incorporates trait data conditioned under a Brownian Motion (BM) model of evolution. We used our size corrected linear measurements plus the first three principal components of variation for the head shape data. We detected sexual dimorphism in our phenotypic data (see Results), therefore we first performed our analyses using only trait data for all the specimens combined and then for each sex separately. Since they gave qualitatively equivalent results we present the results of the runs using all of the specimens. We also performed analyses combining the trait and genomic data with the same  $\theta$  and  $\tau$  prior distribution and same run parameters used for the BPP analyses. For our trait data, we placed uniform priors for the BM control parameters  $\nu$  and  $\kappa$ .

Finally, we applied the recently developed genealogical divergence index (gdi) (Jackson et al., 2017), using the  $\theta$  and  $\tau$  parameter estimates from the MCMC of the BPP analyses using a fixed species tree (Leaché et al., 2018b). The gdi is an estimate of genetic divergence between two taxa (e.g. taxa A and B), in this case calculated as  $1 - e^{-2\tau_{AB}/\theta_A}$ , thus scaling divergence time by population size. Values go between 0 (complete panmixia) and 1 (complete divergence), with values below 0.2 considered strong support for a single species, and above 0.7 strong support for distinct species, whereas values between these two indicate uncertain or ambiguous delimitation (Jackson et al., 2017; Leaché et al., 2018b).

## 2.7. Population structure

To infer genetic structure and the geographic distribution of populations in the *Liolaemus leopardinus* group we used Geneland v. 4.0.8 (Guillot et al., 2005). This program uses molecular and/or phenotypic data to estimate the number of populations in Hardy-Weinberg equilibrium ( $K$ ) and their geographic limits employing an MCMC algorithm. Preliminary analyses using the full biallelic dataset showed poor MCMC mixing and failed to converge after several million generations. Therefore, we reduced our dataset to include 100 unlinked SNPs

**Table 1**

Summary of the BFD\* species delimitation models, including the number of species (excluding the outgroup), the marginal likelihood, the model rank and the Bayes Factor between that model and the model of current taxonomy plus *L. normae* sp. nov. Species in the model description are depicted as abbreviations, as follows: *norma*, *L. normae* sp. nov.; *leo*, *L. leopardinus*; *ramo*, *L. ramonensis*; *valde*, *L. valdesianus*; *uba*, *L. ubaghsi*; *frassi*, *L. frassinettii*.

Model	Species	ML	Rank	BF
Current taxonomy plus <i>norma</i>	6	-8735.87	1	-
Lumped ( <i>leo</i> + <i>ramo</i> )	5	-8896.54	2	-321.34
Lumped ( <i>leo</i> + <i>ramo</i> + <i>valde</i> )	4	-9080.36	3	-688.98
Lumped ( <i>leo</i> + <i>ramo</i> + <i>valde</i> ) and ( <i>uba</i> + <i>norma</i> )	3	-9268.34	4	-1064.94
Lumped ( <i>leo</i> + <i>ramo</i> + <i>valde</i> + <i>frassi</i> )	3	-9550.59	5	-1629.44
Lumped ( <i>leo</i> + <i>ramo</i> + <i>valde</i> + <i>frassi</i> ) and ( <i>uba</i> + <i>norma</i> )	2	-9739.1	6	-2006.46
All lumped	1	-10734.28	7	-3996.82

without missing data. A larger number of loci can cause mixing problems (Guillot, 2012). We coded the SNPs as codominant diploid markers. The geographic coordinates of collecting sites were recorded in the field with a Global Positioning System (GPS) receiver. We ran five independent analyses using the spatially informed and correlated allele frequencies models. Each analysis consisted of one million iterations sampled every 100th, testing  $K$  values between one and ten. We used the run with the highest likelihood with a burnin of 25% to estimate the optimal number and geographic limits of  $K$ .

To infer genetic clustering and admixture we used ParallelStructure (Besnier and Glover, 2013), which runs the program STRUCTURE (Pritchard et al., 2000) in parallel cores, greatly reducing computing time for large datasets. We used the unlinked SNP dataset. We ran the program using the correlated allele frequencies and admixture models, and testing values of  $K$  between one and ten. We ran 10 independent analyses for each value of  $K$ , each consisting of 100,000 burnin generations and 1 million post-burnin generations. Results were summarized and compared in Clumpak (Kopelman et al., 2015). This software facilitates the interpretation of STRUCTURE output by generating graphics using DISTRUCT (Rosenberg, 2004) and estimates the optimal value of  $K$  using the  $\ln \Pr(D|K)$  (Pritchard et al., 2000) and  $\Delta K$  or Evanno (Evanno et al., 2005) methods.

### 3. Results

#### 3.1. Morphometric analyses

Our linear model found a significant effect of species, sex and the interaction between both factors for body shape (species  $F_{(4, 88)} = 7.9$ ,  $P = 0.0001$ ; sex  $F_{(1, 88)} = 3.06$ ,  $P = 0.016$ ; species\*sex  $F_{(4, 88)} = 1.48$ ,  $P = 0.033$ ) and head shape in lateral view (species  $F_{(4, 88)} = 3.34$ ,  $P = 0.0006$ ; sex  $F_{(1, 88)} = 3.12$ ,  $P = 0.003$ ; species\*sex  $F_{(4, 88)} = 1.36$ ,  $P = 0.043$ ) and an effect of species and sex but not of the interaction for head shape in dorsal view (species  $F_{(4, 88)} = 3.44$ ,  $P = 0.0001$ ; sex  $F_{(1, 88)} = 2.72$ ,  $P = 0.016$ ; species\*sex  $F_{(4, 88)} = 0.75$ ,  $P = 0.54$ ). Pairwise comparisons show that most species and the Los Cristales Lagoon sample are phenotypically different from each other (Table S2). However, the PCAs on body and head shape still highlight how morphologically conserved these species are, as their morphospaces largely overlap (Figs. 3 and 4). The variation explained by the principal component (PC) axes of body shape is small, with PC1, PC2 and PC3 only explaining 12.3%, 10.69% and 8.16% of the variation respectively (see Table S3 for details). There is a tendency for *L. ubaghsi* to have larger eyes, wider ear openings, shorter tails and thinner necks, as well as fewer ventral and dorsal scales (Fig. 3). *L. valdesianus* have a tendency towards longer feet and wider necks and *L. frassinettii* towards more dorsal scales and proportionally longer trunks (Fig. 3). The first three PCs of head shape in dorsal view explain more than 80% of the variation (PC1 = 41.3%, PC2 = 24.02% and PC3 = 9.97%), whereas the first three PCs of head shape in lateral view explain 60% of the variation (PC1 = 26.96%, PC2 = 20.15% and PC3 = 12.07%). More structure is observed for head shape in dorsal view than in lateral view

(Fig. 4), but head shape is nevertheless conserved in this clade. The population from Los Cristales Lagoon has a slight tendency for larger eyes and shorter distance between the eyes and ears.

#### 3.2. Phylogenetic hypotheses

With the mtDNA, both the MCC tree from the posterior distribution of the Bayesian analysis and the ML tree supported *Liolaemus frassinettii* as the sister species to the remainder of the *L. leopardinus* clade (Fig. 5). Relationships between the remaining taxa are not well supported in either tree. The population from Los Cristales Lagoon and *L. ubaghsi* are each monophyletic with strong support, but the monophyly of *L. leopardinus*, *L. ramonensis* and of *L. valdesianus* is not supported by either analysis.

The phylogenetic analyses of the SNP data yield contrasting results. The concatenated ML and SVDQuartets trees (Fig. 6) place the Los Cristales Lagoon sample as the sister taxon to the rest of the clade, and within the latter *L. ubaghsi* as the sister of the remaining taxa. Furthermore, *L. frassinettii* is sister to the clade containing the remaining species while *L. valdesianus* is sister to *L. leopardinus* and *L. ramonensis* (which are not reciprocally monophyletic). The trees obtained using both methods are congruent with respect to interspecific relationships, but there are some intraspecific differences (Fig. 6). The species tree inferred by SNAPP differs by inferring the sample from Los Cristales Lagoon as sister to *L. ubaghsi* (Fig. 6).

#### 3.3. Species delimitation

Both GMYC and mPTP identified only two species within the *L. leopardinus* clade: *L. frassinettii*, and a clade consisting of all remaining taxa from the Andes as a single species (Fig. 5). In contrast, the species delimitation analyses using the ddRADseq data display higher numbers of species. The model with the highest marginal likelihood in the BFD\* analysis recognizes each described taxon and the Los Cristales Lagoon sample as distinct species (Table 1). Models with more taxa had higher marginal likelihoods, and the Bayes Factors for every model comparison strongly support the full model with current taxonomy plus the sample from Los Cristales Lagoon.

The BPP and iBPP (combining the ddRADseq and morphological data) analyses using 30 loci and testing a six species model favored the distinction of each taxa with a PP = 0.57 and PP = 0.65 respectively. *Liolaemus frassinettii*, *L. leopardinus*, *L. ubaghsi*, and the sample from Los Cristales Lagoon were each recognized as distinct species with a PP = 1. The split between *L. valdesianus* and *L. ramonensis* + *L. leopardinus* had a PP = 0.99 in BPP and PP = 1 in iBPP. The split between *L. leopardinus* and *L. ramonensis* had a PP = 0.57 in BPP and PP = 0.65 in iBPP. The analysis using 300 loci and collapsing *L. leopardinus*, *L. ramonensis* and *L. valdesianus* a priori favored a four species model with a PP > 0.99 in BPP and PP = 0.72 in iBPP. The sample from Los Cristales Lagoon and *L. ubaghsi* were each recognized with a PP = 1. The split between *L. frassinettii* and *L. leopardinus* ± *L. ramonensis* + *L. valdesianus* had a PP > 0.99 in BPP and PP = 0.72 in iBPP. Finally, in the analysis using

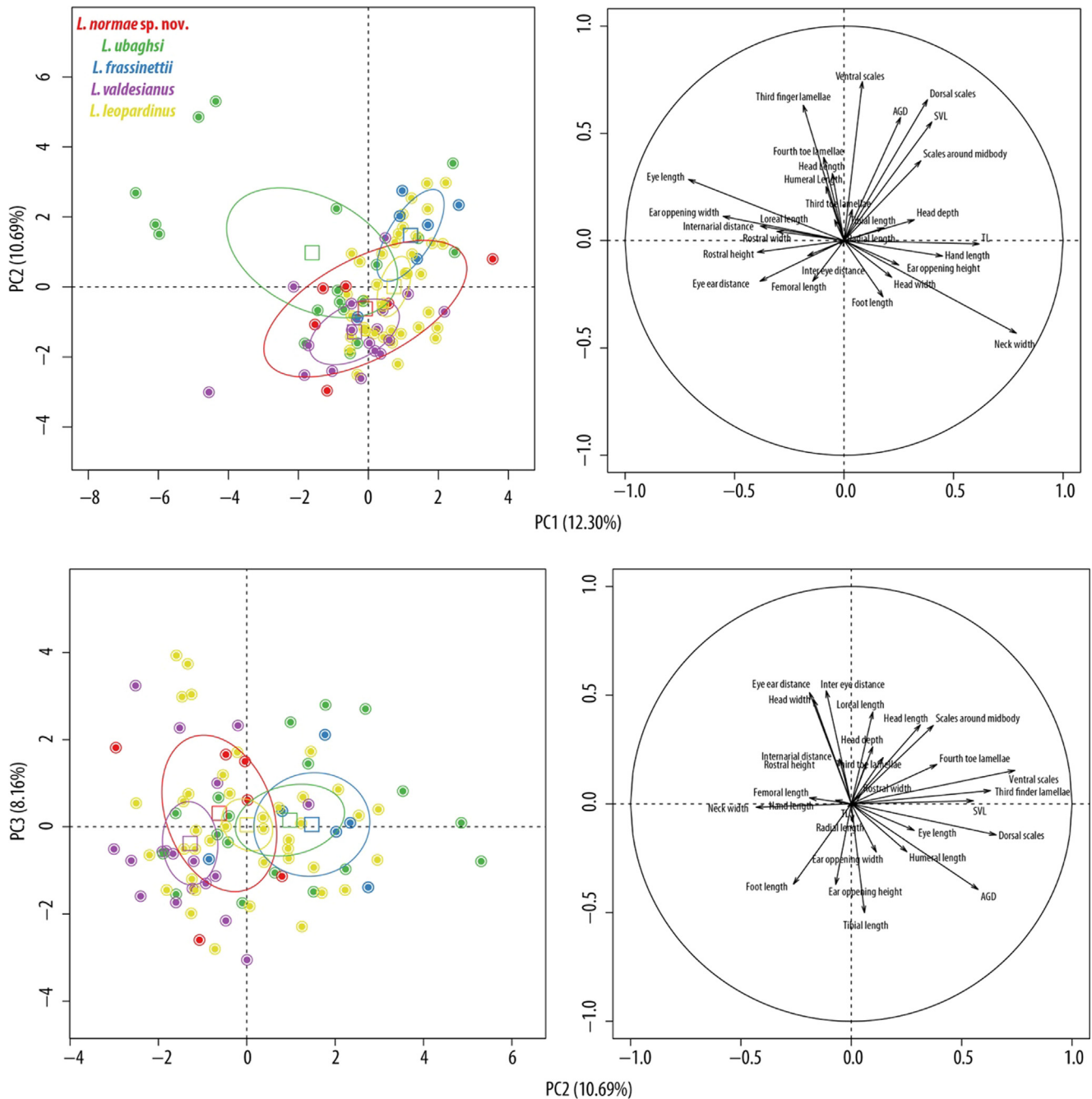


**Fig. 3.** PCA plots for body shape, with PC1 vs PC2 and PC2 vs PC3 on the left and the corresponding variable factor maps which illustrate the variable loadings for each PC, on the right. Points are colored according to species on the legend on the top left and the ellipses correspond to the 95% CI around the centroid of each species. (For interpretation of the references to color in this figure legend, the reader is referred to the web version of this article.)

300 loci and focused in *L. leopardinus*, *L. ramonensis* and *L. valdesianus* a three species model was favored with a PP = 0.96 in BPP and PP = 1 in iBPP. The split between *L. valdesianus* and the other species had a PP = 1 in both, while the split between *L. leopardinus* and *L. ramonensis* had a PP = 0.96 and a PP = 1 in iBPP. In the analysis using phenotypic data only (in iBPP) a model with five species (where *L. ramonensis* and *L. leopardinus* are lumped together) is preferred with PP = 0.77. All the splits are supported with PP = 1, except between *L. leopardinus* and *L. ramonensis* with PP = 0.23.

The gdi (Fig. 7) strongly supports *L. frassinettii* as a genetically distinct species (with a gdi consistently over 0.7), and has ambiguous support for the population from Los Cristales Lagoon, *L. ubaghsi* and *L. valdesianus*. The gdi also suggests *L. ramonensis* and *L. leopardinus* are

the same species, with a gdi below 0.2. See Fig. 8 for a summary of species delimitation results.

### 3.4. Population structure

The five independent runs of Geneland recognized six populations with a posterior probability (PP) of 0.55 (Fig. 9). *Liolaemus frassinettii*, *L. valdesianus*, *L. ubaghsi*, and the sample from Los Cristales Lagoon were all recognized as distinct populations. One specimen of *L. ramonensis* from Cerro Provincia, in the northern portion of the taxon's distribution, was grouped with the samples of *L. leopardinus*. The other samples of *L. ramonensis* comprised a distinct population. The PP of the assignment of each individual to its respective population ranged between

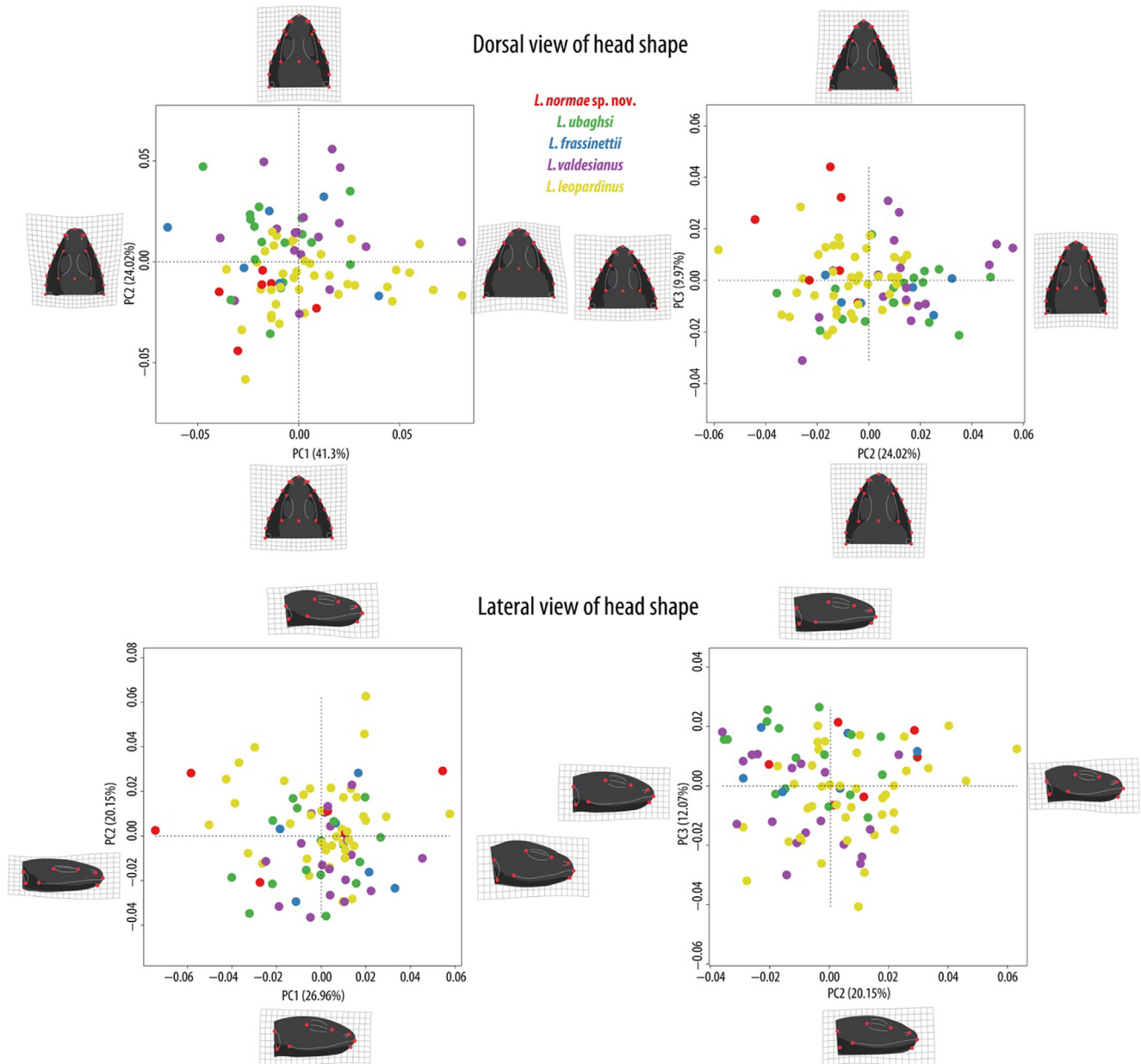


Fig. 4. PCA plots for head shape in dorsal (above) and lateral (below) views. Specimen points are colored according to the legend on the top middle, and PC axis include the percentage of variation they explain. Deformation grids illustrate the specimens at the extreme variability at each axis.

0.32 in the individuals of *L. ubaghshi* and 0.45 in the single sample of *L. frassinettii*.

The results obtained with STRUCTURE are summarized in Fig. 10. The value of  $K$  peaked at six using the  $\ln \Pr(D|K)$  method and at three using the  $\Delta K$  method. In the six population model, *Liolaemus frassinettii*, *L. leopardinus*, *L. ubaghshi*, and the sample from Los Cristales Lagoon were easily distinguished from each other and showed low levels of admixture. On the other hand, the individuals of *L. ramonensis* and *L. valdesianus* showed high levels of admixture with respect to *L. leopardinus*. The estimated admixture was low in the three population model. In that model, *L. frassinettii* was easily distinguished from the other taxa, *L. ubaghshi* and the sample from Los Cristales Lagoon were clustered together, and *L. leopardinus*, *L. ramonensis* and *L. valdesianus* were considered a single population. Visual exploration of the DISTRUCT bar plots revealed that a value of  $K = 4$  is the maximum value of  $K$  at which population structure is clearly discernible and admixture minimal. In the four population model *L. frassinettii*, *L. ubaghshi*, and the

sample from Los Cristales Lagoon conformed distinct clusters. On the other hand, *L. leopardinus*, *L. ramonensis* and *L. valdesianus* were clustered together.

### 3.5. Taxonomy

We recognize five species in the *L. leopardinus* clade based on the following criteria: reciprocal monophyly, distinction by most species delimitation and population structure methods, morphological diagnosability, and geographic distributions that make gene flow extremely unlikely. We recognize the population of Los Cristales Lagoon as a distinct species, which we describe below. We also conclude that *L. ramonensis* is not an independent evolutionary lineage with respect to *L. leopardinus* and we relegate *L. ramonensis* to a junior synonym of *L. leopardinus*.

*Liolaemus normae* sp. nov.

*Holotype*. SSUC-Re 738, male, collected at Los Cristales Lagoon



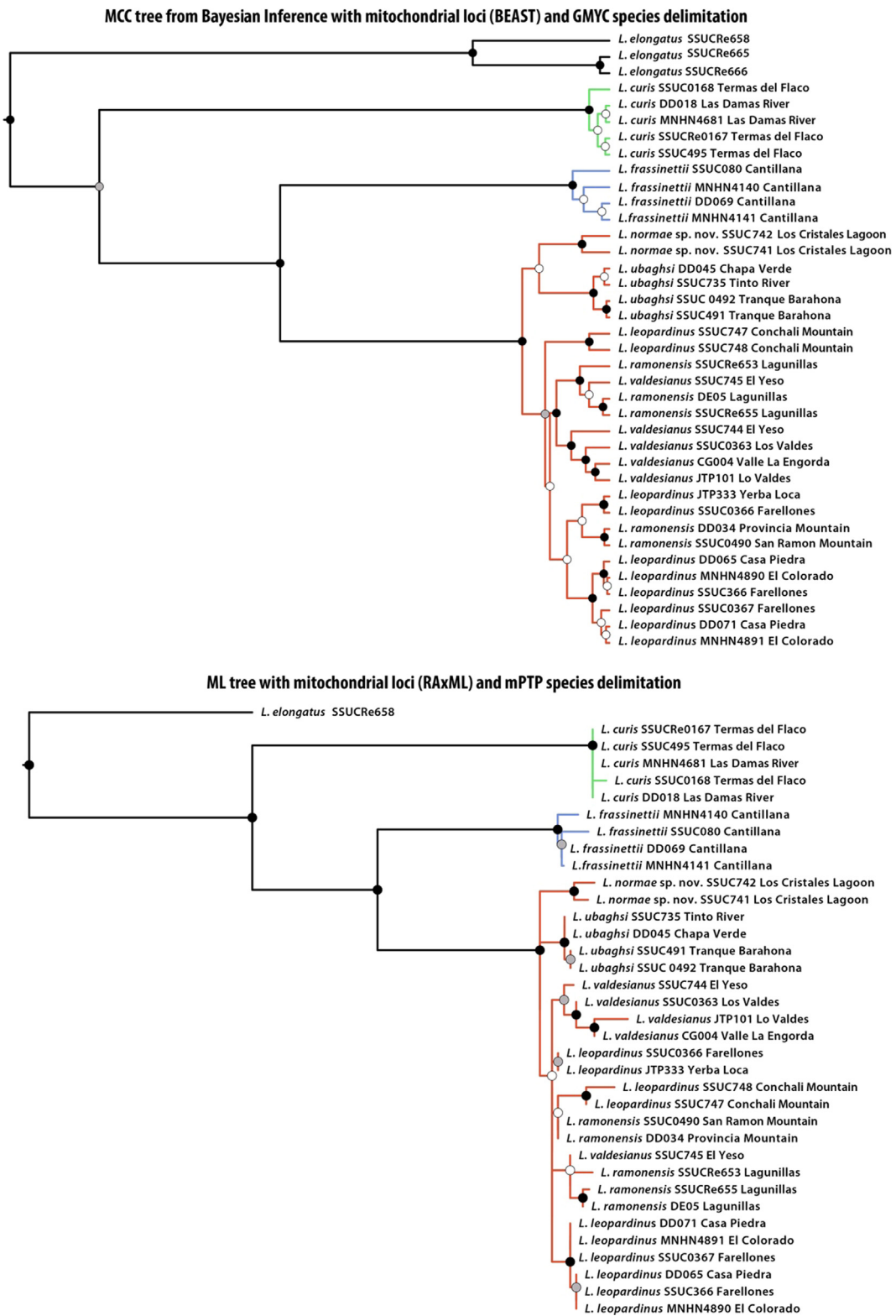


Fig. 5. Above: MCC tree from the posterior MCMC chain of the Bayesian phylogenetic inference ran on BEAST 2 using the mitochondrial loci. Black nodes indicate a posterior probability (PP) over 0.95, gray nodes indicate a pp between 0.95 and 0.8, and white nodes indicate pp below 0.8. Colored clades correspond to species identified by GMYC. Below: ML tree inferred by RAxML using the mitochondrial loci with RAxML. Black nodes indicate a bootstrap support over 80%, gray nodes indicate a bootstrap support between 80% and 50%, and white nodes indicate bootstrap support below 50%. Colored branches correspond to species identified by mPTP. (For interpretation of the references to color in this figure legend, the reader is referred to the web version of this article.)

(34°34'10"S – 70°31'05"W), Rengo, O'Higgins Region, Chile, at 2,372 m, by Diego Ramírez-Álvarez and Jaime Troncoso-Palacios, on January 21, 2016. See Fig. S1.

Paratypes. SSUC-Re 739, male; SSUC-Re 740, male; and SSUC-Re 743, female. Same collection data as holotype, 2279–2372 m. SSUC-Re 741, female; SSUC-Re 742, male; same locality as the

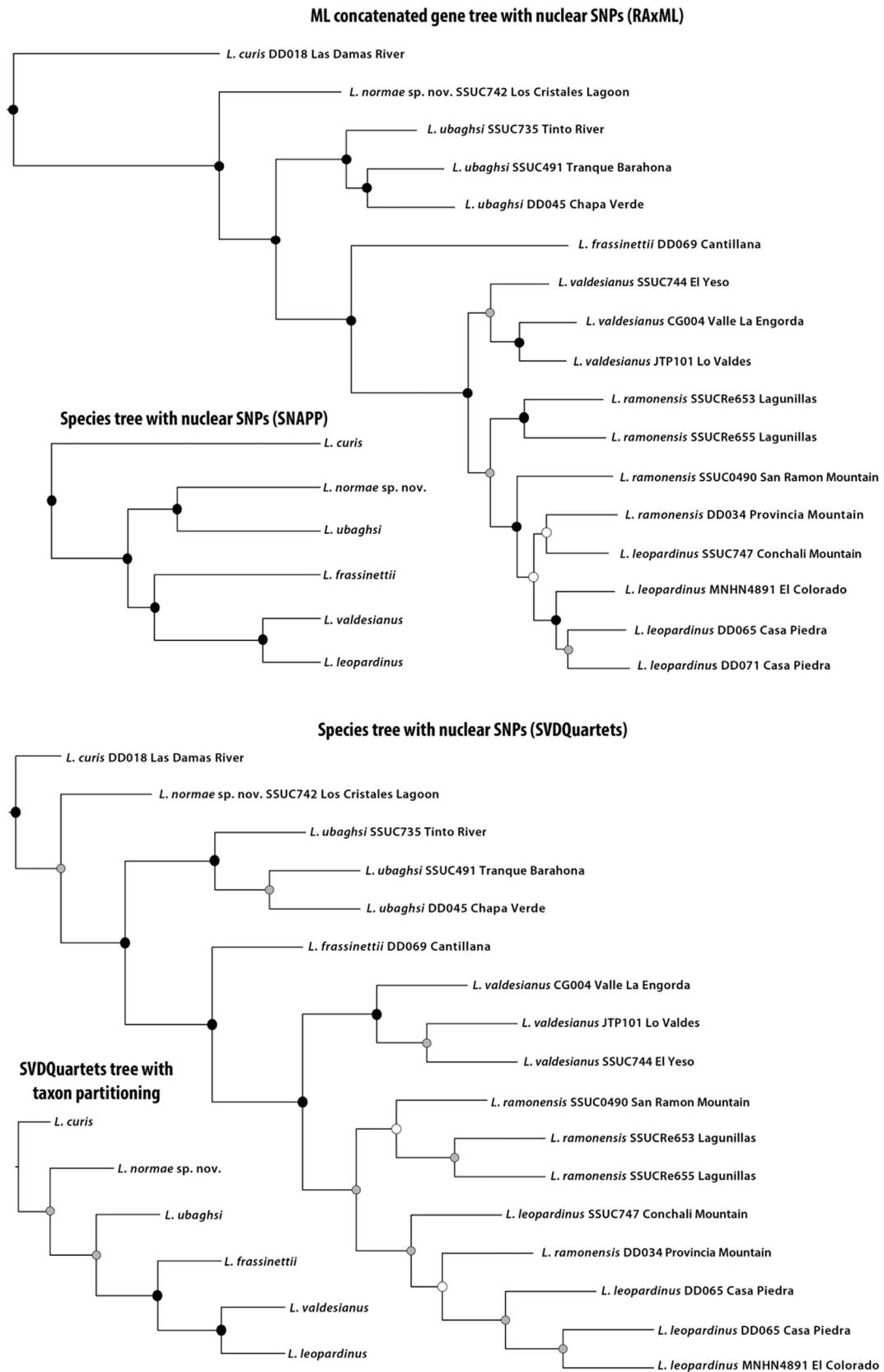


Fig. 6. Phylogenetic hypotheses inferred with SNPs. Above the ML tree inferred by the concatenated full ddRADseq loci using RAxML, and SNAPP tree using the biallelic unlinked SNP dataset. Below the species tree based on the biallelic unlinked SNPs using SVDQuartets and the SVDQuartets species tree using the taxon partitioning based on monophyletic lineages. Bootstrap details as in Fig. 5.

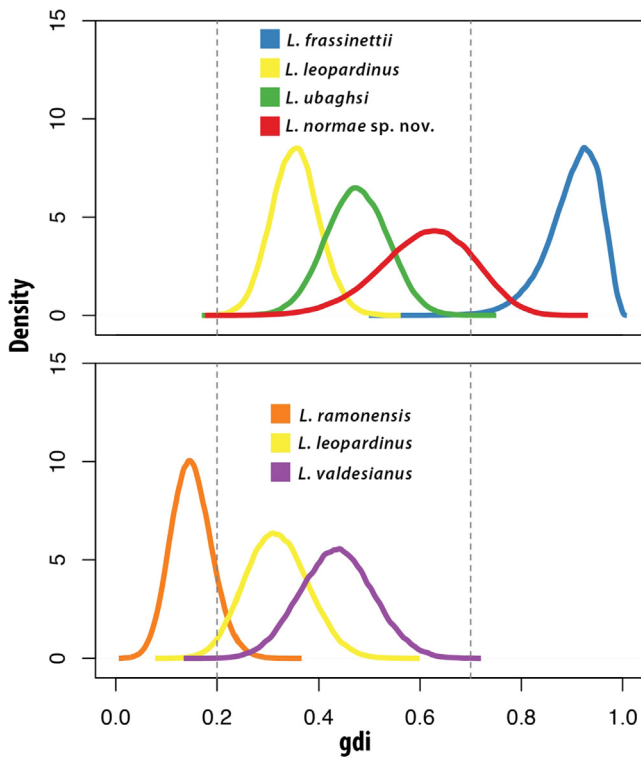


Fig. 7. Posterior distribution of genealogical divergence indexes (gdi) estimated from the BPP parameters with the analysis collapsing *L. leopardinus*, *L. valdesianus* and *L. ramonensis* (above) and only focusing on those three taxa (below).

holotype, collected by Diego Ramírez-Álvarez on March 28, 2015.

See Fig. S2.

**Diagnosis.** The most conspicuous diagnostic trait that allows *L. normae* sp. nov. to be differentiated from all the other member of the *L. leopardinus* clade is its deep blood red belly (Figs. 11 and S3). It differs from *L. leopardinus* in completely lacking the leopard-like spots characteristic of this species. Despite both having dark flanks, *L. normae* sp. nov. differs from *L. frassinettii* and *L. valdesianus* by not having a black post-humeral spot that ends around mid-body and by not having leopard-like spots on the tail. We could not find consistent scalation traits that would serve to distinguish it from the other species. See Table S4 for morphological comparison between taxa.

**Description.** Medium sized lizard (max. SVL 88.76 mm). Body measurements and scale counts of the holotype and paratypes can be seen in

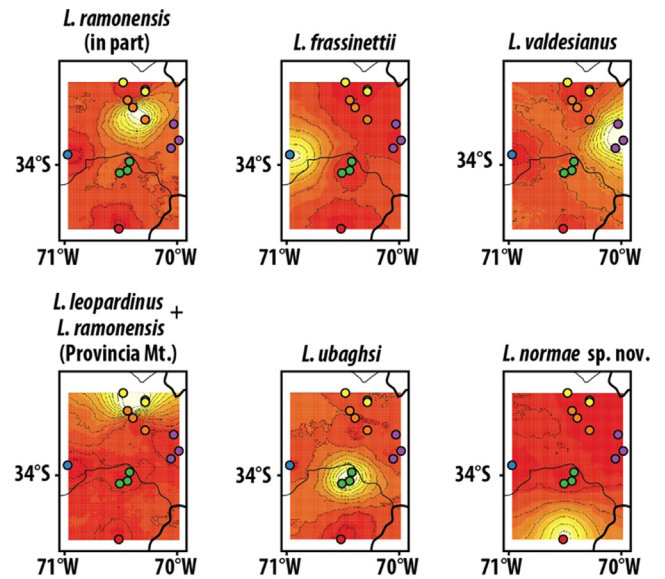


Fig. 9. Geneland results displaying the number of populations and probability of assignment of individuals to populations. Colors closer to white represent higher probability and closer to red represent lower probability. (For interpretation of the references to color in this figure legend, the reader is referred to the web version of this article.)

Table S5. The neck is usually as wide or wider than the head due to prominent neck folds. General dorsal coloration is dark brown, with a darker head and flanks. It also has a faint mid-dorsal stripe with a similar but slightly lighter coloration as the flanks and head. Some specimens have very faint, darker transverse bars along the dorsum, on each side of the mid-dorsal stripe. The dorsal surface of tail is same color as dorsum, with dark antero-posteriorly elongated spots, around 4 scales long and separated from each other by another four scales, which become darker and more defined towards the tip of the tail. Hollow or leopard-like spots, common within the *L. leopardinus* clade, are never present in *L. normae* sp. nov. Sometimes white, one-scale sized dots are on the dorsal surface of the femoral area and on top of the first third of the tail. The background coloration on the ventral side is gray, with dark gray spots scattered evenly. The belly is consistently blood red, with variation on the degree of red pigmentation on the cloacal region, hind-limbs and tail. Some specimens display red pigmentation on the front limbs and ventral surface of the head, but it is always less pronounced than in the belly. See Fig. S4 for photographs of live specimens. Rostral scale is rectangular, in contact with eight scales,

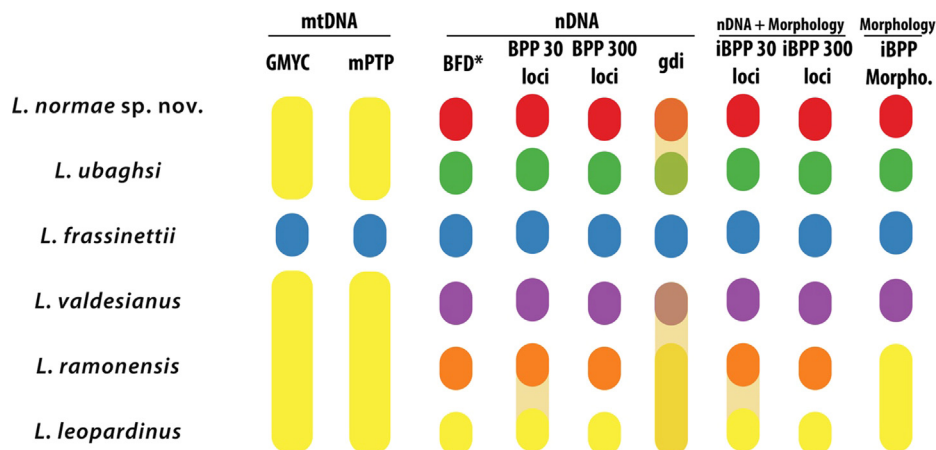


Fig. 8. Summary of the species delimitation analyses. For each analysis, blocks of the same color represent lineages that have been inferred as the same species. Faint areas connecting blocks indicate that the support for the split between those taxa is low (PP < 0.8 in BPP and iBPP and gdi between 0.2 and 0.7 in gdi).

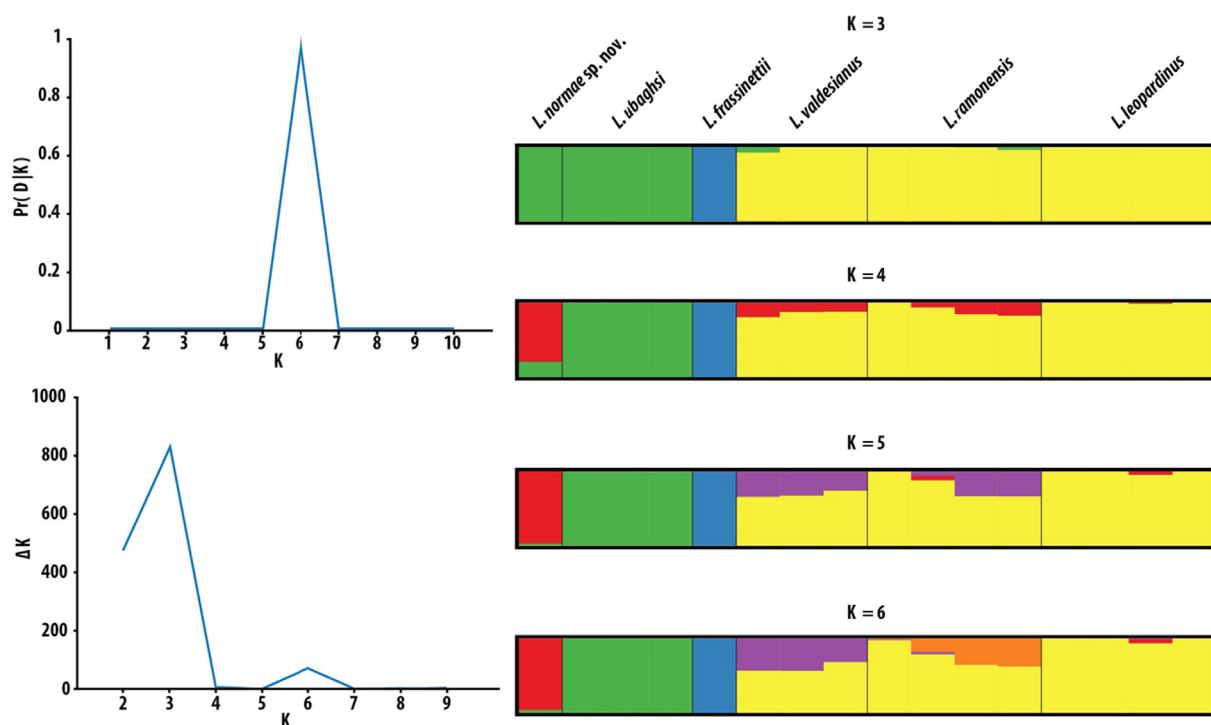


Fig. 10. Bayesian genetic clustering of the 16 individuals using the program *STRUCTURE*. The profiles for the two optimal numbers of clusters or populations ( $K$ ) inferred using two methods ( $\ln \text{Pr}(D|K)$  and  $\Delta K$ ) are shown on the left.

including the nasal scales. Nostrils occupy around half of the nasal scales, on their posterior side. It has two post-rostral and four internasals scales. Between six and ten irregular frontonasal scales. Two prefrontal scales, with a frontal ranging from undivided to divided into three smaller scales. Two to four post-frontal scales, normally irregular in shape. Whitish pineal eye in the middle of the interparietal scale. Interparietal scale is pentagonal, the tip facing posteriorly and in contact with usually six but up to nine scales. Normally two but sometimes four parietal scales. Occipital scales irregular, juxtaposed and smooth. Supratemporal scales similar to occipitals but larger. Between five and seven large supraocular shields, with 16–22 smaller supraocular scales. Five to seven loreal scales. One row of lorilabial scales. Six to seven superciliary scales. Six to eight supralabial scales, with the fourth one curved upwards. Between 12 and 17 superior and 14–17 inferior palpebral scales. Temporal scales roughly hexagonal and slightly keeled. Mental scale as wide or wider than rostral, in contact with four scales. Four to five pairs of postmental shields. Gular scales rounded, overlapping and smooth. Neck scales are granular. Dorsal scales triangular or subtriangular, slightly overlapping or juxtaposed and keeled. Between 67 and 81 dorsal scales, between the occipital area and the anterior edge of the thighs. There is a longitudinal skin fold between the armpit and the groin. Between 80 and 93 scales around mid-body. Lateral scales are subtriangular, slightly keeled, and become progressively smoother towards the ventrum. Ventral scales rounded, smooth and overlapping, similar sized or slightly larger than dorsal scales. Between 108 and 128 ventral scales between the mental scale and the cloaca. Males have three small, orange precloacal pores. Suprabrachial scales triangular, keeled and overlapping. Supraantibrachial scales subtriangular, keeled and overlapping. Infrabrachial scales granular, smooth, juxtaposed and small interstitial granules in between. Infrantibrachial scales subtriangular and overlapping, smooth on the anterior edge and keeled towards the posterior edge. Suprametacarpal scales subtriangular to rounded, and overlapping, the anterior ones are smooth and posteriorly they become slightly keeled. Inframetacarpal scales slightly are keeled, overlapping and with a jagged edge. Supradigital scales of manus smooth, wider than long and overlapping.

Infradigital lamellae of manus wider than long, overlapping and with three keels. Between 19 and 21 lamellae on the third finger (counting from the inside out, dorsally). Strong, curved and brown claws. Suprafemoral scales subtriangular, smooth on the anterior edge and keeled on the dorsal surface. Posteriorly they become granular. Supratibial scales subtriangular and keeled, slightly overlapping or juxtaposed. They become smaller and even granular towards the foot. Supratarsal scales subtriangular to triangular, keeled and overlapping. Infracarpal scales rounded, smooth and overlapping, with a patch of granular scales on the anterior side. Infracarpal scales rounded, smooth and overlapping. Infracarpal scales overlapping and keeled, with a jagged edge. Supradigital scales of foot keeled, wider than long and overlapping. Infradigital lamellae of foot wider than long, with three keels and overlapping. Between 23 and 26 lamellae on the third toe (counting from the inside out, dorsally) and 28–31 lamellae on the fourth toe. Supracaudal scales triangular, keeled and overlapping. Infracaudal scales triangular to subtriangular, smooth and overlapping.

**Natural History.** This lizard is diurnal and lives in rocky outcrops in high Andean habitat. Just like all of the species in the *L. leopardinus* and *L. elongatus* clades and most *Liolaemus* adapted to high altitudes, *L. normae* sp. nov. is probably viviparous. It lives in sympatry with *L. schroederi* Müller & Hellmich, 1938, *L. curicensis* Müller & Hellmich, 1938 and *Phymaturus maulense* Núñez, Veloso, Espejo, Veloso, Cortes & Araya, 2010. The vegetation is characterized as Andean low scrubland (Luebert and Plissock, 2006), dominated principally by shrubs of *Senecio* sp., and herbs like *Vigueira revoluta* and *Mimulus glabratus*. The species has a saxicolous behavior, and is generally found near water.

**Distribution.** It is currently only known from its type locality, Los Cristales Lagoon, between 2300 and 2500 m above sea level (Fig. S5). This lagoon has an area of 240 ha, and is fed by four mountain creeks coming from nearby glaciers. Further exploration of close Andean areas might reveal a more wide-spread population.

**Etymology.** Dedicated to Norma Álvarez, mother of DRA (who discovered the population in Los Cristales Lagoon). We propose the common names “Los Cristales leopard lizard” or “Norma’s leopard lizard” in English and “lagarto leopardo de Los Cristales” or “lagarto

leopardo de Norma” in Spanish.

#### 4. Discussion

This study highlights the importance of exploring different lines of evidence when establishing phylogenetic histories and taxonomic boundaries, especially in rapidly diverging systems like *Liolaemus*. We show how reliance on a single locus (mtDNA) can lead to conclusions that conflict with inferences made using multiple independent loci. Gene tree discrepancies are expected in organisms with shallow divergences and that likely have considerable levels of incomplete lineage sorting and/or introgression (Kutschera et al., 2014; Toews and Brelsford, 2012). The mtDNA genealogies support a different evolutionary history and different species limits than our multi-locus species trees. We first discuss the utility of multi-locus species delimitation methods and the possible causes of gene tree/species tree discordance in the *L. leopardinus* clade, followed by the likely role of Pleistocene glaciation cycles on the evolution and diversification of *Liolaemus* in the Andes.

##### 4.1. Species delimitation

Despite the recent progress in species delimitation using genetic data (Fujita et al., 2012; Leaché et al., 2018b; Luo et al., 2018), taxonomists are still required to make qualitative judgments based on different lines of evidence to decide on the boundary between populations and species (Sites and Marshall, 2004). Following single lines of evidence, such as a single locus, can lead to idiosyncratic results (Jackson et al., 2017; Sukumaran and Knowles, 2017), hence the need to follow integrative approaches when delimiting species. The single locus species delimitation methods we performed using mtDNA suggest all leopard lizards, except for *L. frassinettii*, belong to the same species (Fig. 5). However, there is considerable evidence from other sources of data supporting more than two species in the *L. leopardinus* group. First, the populations are allopatric, separated from each other by one or several low-altitude river valleys that act as biological barriers. Second, these species are morphologically easily distinguishable, at least by their dorsal patterns (Figs. 11 and S3). Third, the ddRADseq data suggests multiple species in the group (Figs. 6–8). Fourth, integrative species delimitation combining the multi-species coalescent and morphology consistently support multiple (five to six) independent evolutionary lineages (Fig. 8), and finally, there are at least four genetic clusters with little to no evidence of admixture (Figs. 9 and 10). Our analyses support at least five unique species, which includes one new species herein named *Liolaemus normae* sp. nov., and the taxonomic sinking of *L. ramonensis*.

*L. leopardinus* and *L. ramonensis* are not reciprocally monophyletic with either mtDNA or SNPs. This lack of support, and the consistent results suggesting that they belong to a single genetic cluster, leads us to conclude that they do not represent independent evolutionary lineages. Furthermore, these taxa differ only by having slight differences in color pattern (Fig. 11), which may simply reflect local adaptation or be a product of neutral evolution with somewhat limited gene flow. Therefore, we relegate *L. ramonensis* to a junior synonym of *L. leopardinus*. The status of *L. valdesianus* remains uncertain. Even though we find strong support for a distinct species based on species delimitation analyses (Fig. 8), population structure analysis reveals extensive admixture with *L. leopardinus* (Fig. 10). Future studies aimed specifically at introgression between these taxa are required to clarify this.

Species delimitation methods based on single loci are a controversial tool to assess the boundaries between species (Fujisawa and Barraclough, 2013; Hickerson et al., 2006; Yang and Rannala, 2017). Given that they rely on the topology inferred from a single locus while assuming that it represents the correct species relationships, incorrect topologies due to introgression and/or incomplete lineage sorting can render these methods misleading (Dupuis et al., 2012; Knowles and

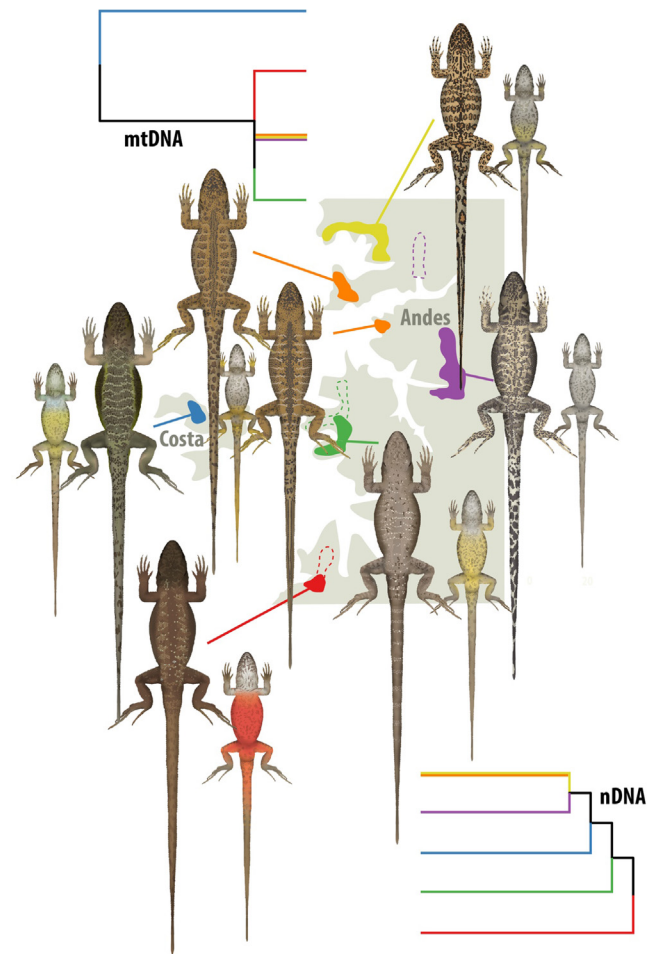


**Fig. 11.** Schematic showing the dorsal (larger) and ventral (smaller) pattern variation and distribution among populations and taxa of the *Liolaemus leopardinus* clade. Additionally, on the top left corner and the bottom right corner we have included the topologies inferred from the mtDNA and SNPs, respectively, where a branch with multiple colors represents no reciprocal monophyly for those taxa. Colors follow previous figures. (For interpretation of the references to color in this figure legend, the reader is referred to the web version of this article.)

Carstens, 2007; Luo et al., 2018). These methods should be taken with extreme caution in systems where these phenomena are likely to be happening. Recent studies have demonstrated that introgression and incomplete lineage sorting are far more common than previously thought (Mallet, 2005; McGuire et al., 2007; Olave et al., 2018). For example, polar bears were inferred by mtDNA as a recent lineage of brown bears that adapted to arctic conditions (Edwards et al., 2011), but multi-locus nuclear data later revealed they are a much older and independent evolutionary lineage (Hailer et al., 2012). Methods that incorporate multi-locus data in a multi-species coalescent framework, that take into account incomplete lineage sorting and are robust to low levels of introgression (Zhang et al., 2011) have revolutionized the field of phylogenetic systematics (Welton et al., 2013). Multi-species coalescent based methods like BPP have been empirically shown to outperform single-locus methods like GMYC and PTP in delimiting species (Luo et al., 2018), which also tend to be discordant between them (Blair and Bryson, 2017).

##### 4.2. Reproductive isolation

*Liolaemus* are a rapidly diversifying group (Esquerré et al., 2019; Pincheira-Donoso et al., 2015), and incomplete lineage sorting and

introgression make elucidating the phylogenetic history of many groups of *Liolaemus* extremely challenging (Grummer et al., 2018; Morando et al., 2004; Olave et al., 2018, 2011). Introgression between *Liolaemus* species might be very common (Olave et al., 2018), although it has so far only been reported in the *L. fitzingeri*, *L. boulengeri* and *L. rothi* complexes (Grummer et al., 2018; Olave et al., 2018) from Argentinean Patagonia. The lack of strong geographic barriers in topographically simple regions like eastern Patagonia could promote hybridization. The allopatric distributions of Andean taxa in the *L. leopardinus* clade make contemporary gene flow very unlikely. However, lineages evolving via genetic drift in geographic isolation are unlikely to experience strong reinforcement for reproductive isolation mechanisms (Safraan et al., 2013). Thus, when these previously isolated lineages come into secondary contact, hybridization is a logical consequence, despite being on independent evolutionary trajectories.

The *L. leopardinus* clade originated during the Pleistocene, approximately 1–3 million years ago (Esquerré et al., 2019). Pleistocene glacial cycles, by expanding, contracting and shifting species distribution, are known to have acted as speciation pumps by promoting repeated reproductive isolation (April et al., 2013; Johnson and Cicero, 2004). Such distributional rearrangements also could lead to secondary contact between previously isolated populations (Fussi et al., 2010; Hewitt, 1996). It has been proposed that glacial periods drive Andean taxa to lower altitudes, and interglacial periods force them to retreat back to mountain tops, promoting a cycle of possible hybridization events during glacial periods and complete allopatry during interglacial periods (Fuentes and Jaksic, 1979). The harsh topographic complexity of the Andes in central Chile likely promoted allopatry by preventing gene flow between populations of high-altitude adapted, low-dispersal liolaemid lizards, but periods of historical secondary contact during glacial maxima might explain the mito-nuclear discordance observed in this study.

#### 4.3. Phylogenetic discordance

The most conspicuous discordance between the mtDNA and SNPs datasets is the placement of *L. frassinettii* as sister to all other taxa in the mtDNA gene trees (Fig. 5), and as sister to the northern Andean lineages in the SNP trees (Fig. 6). *L. frassinettii* is the only taxon found in the parallel Costa Cordillera, and therefore the most geographically isolated from the rest. The Andes are separated from the Costa Cordillera by a valley that reaches 500 m in elevation, over 1000 m lower than the lowest records of leopard lizards. The gene tree/species tree discordance is most likely due to past introgression between the Andean lineages, likely during glacial periods where high altitude species might have shifted to lower altitudes, permitting secondary contact (Fuentes and Jaksic, 1979). This would explain why the mitochondrial genealogy infers the Andean species as a clade, sister to the Cordillera de la Costa taxon (Fig. 11), and this taxon has the highest gdi (Fig. 7) and displays lowest level of admixture (Fig. 10). Moreover, the species trees suggest that the leopard lizards originated south of their current distribution, and have been splitting into lineages as they progressively dispersed north. This is further supported by the fact that the sister species to the *L. leopardinus* clade (according to mtDNA and ddRADseq data) is *L. curis*, from the Tinguiririca River, which is further south than any record of the *L. leopardinus* clade. Additionally, the *L. leopardinus* clade is part of the *L. elongatus-kriegi* complex, which has a southern Andes or Patagonian origin (Esquerré et al., 2019). Leopard lizards likely originated in the south-central Andes of Chile, and have been progressing north. At some point, likely at a glacial maximum that allowed a shift to lower elevations, the lineage represented by *L. frassinettii* dispersed to the Costa Cordillera and subsequently remained isolated, while some introgression occurred between the Andean lineages.

#### 4.4. Closing remarks

Despite a commonly perceived ‘rivalry’ between morphology and genetic based systematics (Page et al., 2005), we argue that both lines of evidence ideally should be considered when establishing species limits. Even though we find statistical support for a morphometric differentiation between our taxa, body and head shape and meristic traits like scale counts remain very conserved in the *L. leopardinus* clade (Figs. 3 and 4), a pattern frequently found in nature (Pfenninger and Schwenk, 2007). The evolutionary diversity of this group is more finely revealed by molecular data. Low rates of phenotypic evolution can be attributed to niche conservatism (Smith et al., 2011), and indeed all species of this clade display a very similar ecology, living in high elevation Andean rocky environments. Nevertheless, dorsal pattern differences (Fig. 11), still play a crucial role in diagnosing and identifying species in this clade.

We provide the most comprehensive molecular phylogenetic analysis of the *Liolaemus leopardinus* clade, which is a true logistical and physical challenge given their restrictive distribution in the high Andes. There are populations only known from photographs like Rio Olivares Park, Rio Clarillo National Reserve and Rio Cipreses National Reserve (Diaz et al., 2002; Diaz and Simonetti, 1996; Esquerré et al., 2014; Esquerré and Núñez, 2017). We can only speculate that these belong to *L. valdesianus*, *L. ubaghsi* and *L. normae* sp. nov. respectively, based on geography and what little we can see in the photographs. Future efforts should aim at further exploring the hard-to-access Andean regions of central Chile and Argentina to have a better understanding of the level of genetic connectivity between these taxa.

Even though many studies in *Liolaemus* systematics still rely solely on morphology or single genetic markers, researchers have been shifting to more integrative approaches, considering multiple lines of evidence (e.g. Aguilar et al., 2016; Minoli et al., 2014). The data presented in this study highlights the importance of incorporating multi-locus and other data (i.e. morphology, ecology) to study phylogenetics and systematics in challenging systems such as Andean *Liolaemus*. We also add to the growing body of evidence that ddRADseq is a useful genomic tool for delimiting species with varying levels of divergence (Herrera and Shank, 2016; Leaché et al., 2014; Shaffer et al., 2007).

#### Acknowledgements

We thank Angel Esquerré and Trinidad Zegers for assistance in collecting the morphometric data. We thank Herman Núñez (MNHN) and Patricio Zavala (SSUC) for facilitating the examination of specimens under their care. We thank Emmanuel A. Pavón Vázquez for IT support and Alison Gonçalves Nazareno for suggestions on running Geneland. We thank Paula Silva and Ivan Salgado for help in the field, and Marcia Ricci for identifying the plant species found. DE is supported by a Becas Chile-Conicyt scholarship. JTP thanks Mario Penna (Universidad de Chile) for his support. JSK thanks the Australian Research Council for ongoing support. We thank CONAF (Corporación Nacional Forestal) and SAG (Servicio Agrícola y Ganadero) for collecting permits N° 1692/2015 and N° 142/2017.

#### Appendix A. Supplementary material

Supplementary data to this article can be found online at <https://doi.org/10.1016/j.ympev.2019.106524>.

#### References

- Abdala, C.S., Quinteros, A.S., 2014. Los últimos 30 años de estudios de la familia de lagartijas más diversa de Argentina. Actualización taxonómica y sistemática de Liolaemidae. Cuad. Herp. 28, 55–82.
- Abdala, C.S., Quinteros, A.S., Scrocchi, G.S., Stazzonelli, J.C., 2010. Three new species of the *Liolaemus elongatus* group (Iguania: Liolaemidae) from Argentina. Cuad. Herp. 24, 93–109.







- 02200.x.
- Shaffer, H.B., Thomson, R.C., Weins, J., 2007. Delimiting species in recent radiations. *Syst. Biol.* 56, 896–906. <https://doi.org/10.1080/10635150701772563>.
- Sites, J.W., Marshall, J.C., 2004. Operational criteria for delimiting species. <https://doi.org/10.1146/annurev.ecolsys.35.112202.130128>.
- Smith, K.L., Harmon, L.J., Shoo, L.P., Melville, J., 2011. Evidence of constrained phenotypic evolution in a cryptic species complex of agamid lizards. *Evolution* 65, 976–992. <https://doi.org/10.1111/j.1558-5646.2010.01211.x>.
- Solis-Lemus, C., Knowles, L.L., Ané, C., 2015. Bayesian species delimitation combining multiple genes and traits in a unified framework. *Evolution* 69, 492–507. <https://doi.org/10.1111/evo.12582>.
- Spehn, E.M., Rudmann-Maurer, K., Körner, C., 2011. Mountain biodiversity. *Plant Ecol. Divers* 4, 301–302. <https://doi.org/10.1080/17550874.2012.698660>.
- Stamatakis, A., 2014. RAxML version 8: a tool for phylogenetic analysis and post-analysis of large phylogenies. *Bioinformatics* 30, 1312–1313. <https://doi.org/10.1093/bioinformatics/btu033/-/DC1>.
- Sukumaran, J., Knowles, L.L., 2017. Multispecies coalescent delimits structure, not species. *Proc. Natl. Acad. Sci. USA* 114, 1607–1612. <https://doi.org/10.1073/pnas.1607921114>.
- Swofford, D.L., 2003. Paup\*. Phylogenetic analysis using parsimony (\* and other methods). Version 4.
- Toews, D.P.L., Brelsford, A., 2012. The biogeography of mitochondrial and nuclear discordance in animals. *Mol. Ecol.* 21, 3907–3930. <https://doi.org/10.1111/j.1365-294X.2012.05664.x>.
- Troncoso-Palacios, J., Díaz, H.A., Esquerré, D., Urra, F.A., 2015. Two new species of the *Liolaemus elongatus-kriegi* complex (Iguania, Liolaemidae) from Andean highlands of southern Chile. *ZooKeys* 500, 83–109. <https://doi.org/10.3897/zookeys.500.8725>.
- Uetz, P., Hošek, J., 2014. The reptile database. Available at < <http://www.reptile-database.org> > . Accessed September 1, 2018 [WWW Document]. < <http://www.reptile-database.org> > . URL (accessed 1.8.17).
- Vuilleumier, F., 1970. Insular biogeography in continental regions. I. The northern Andes of South America. *Am. Nat.* 104, 378–388.
- Warren, D.L., Geneva, A.J., Lanfear, R., 2017. RWTY (R We There Yet): An R package for examining convergence of Bayesian phylogenetic analyses. *Mol. Biol. Evol.* 34, 1016–1020. <https://doi.org/10.1093/molbev/msw279>.
- Weitschat, W., 2016. Intraspecific variation of *Svalbardiceras spitzbergensis* (Frebald) from the Early Triassic (Spathian) of Spitsbergen. *Polar Res.* 27, 292–297. <https://doi.org/10.1111/j.1751-8369.2008.00041.x>.
- Welton, L.J., Siler, C.D., Oaks, J.R., Diesmos, A.C., Brown, R.M., 2013. Multilocus phylogeny and Bayesian estimates of species boundaries reveal hidden evolutionary relationships and cryptic diversity in Southeast Asian monitor lizards. *Mol. Ecol.* 22, 3495–3510. <https://doi.org/10.1111/mec.12324>.
- Yang, Z., 2015. The BPP program for species tree estimation and species delimitation. *Curr. Zool.* 61, 854–865.
- Yang, Z., Rannala, B., 2017. Bayesian species identification under the multispecies coalescent provides significant improvements to DNA barcoding analyses. *Mol. Ecol.* 26, 3028–3036. <https://doi.org/10.1111/mec.14093>.
- Yang, Z., Rannala, B., 2010. Bayesian species delimitation using multilocus sequence data. *Proc. Natl. Acad. Sci. U.S.A.* 107, 9264–9269. <https://doi.org/10.1073/pnas.0913022107>.
- Zhang, C., Zhang, D.-X., Zhu, T., Yang, Z., 2011. Evaluation of a Bayesian coalescent method of species delimitation. *Syst. Biol.* 60, 747–761. <https://doi.org/10.1093/sysbio/syr071>.